THE JOURNAL OF BIOLOGICAL CHEMISTRY VOL. 289, NO. 36, pp. 24911–24921, September 5, 2014

Structural and Functional Studies of the Modulator NS9283 Reveal Agonist-like Mechanism of Action at $\alpha4\beta2$ Nicotinic Acetylcholine Receptors*

Received for publication, March 24, 2014, and in revised form, June 24, 2014 Published, JBC Papers in Press, June 30, 2014, DOI 10.1074/jbc.M114.568097

Jeppe A. Olsen[‡§¶1], **Philip K. Ahring**[¶‖], **Jette S. Kastrup**[§], **Michael Gajhede**[§], **and Thomas Balle**[¶2]

From [‡]*NeuroSearch A/S, Pederstrupvej 93, 2750 Ballerup, Denmark, the* [§]*Faculty of Health and Medical Sciences, University of Copenhagen, 2100 Copenhagen, Denmark, the* [¶]*Faculty of Pharmacy, The University of Sydney, Sydney, New South Wales 2006, Australia, and* [‖]*Saniona AB, Baltorpvej 54, 2750 Ballerup, Denmark*

Background: Cys loop receptors can be modulated by exogenous compounds.
Results: By combining x-ray crystallography, homology modeling, quantum mechanical calculations, and functional studies on $\alpha4\beta2$ nAChRs, the binding mode and modulatory mechanism of the $\alpha4\beta2$ nAChR modulator NS9283 were revealed.
Conclusion: Modulatory actions occur by mimicking agonists in the $\alpha4$-$\alpha4$ ACh-binding pocket.
Significance: Increased understanding of modulator actions open new possibilities for rational drug design.

Modulation of Cys loop receptor ion channels is a proven drug discovery strategy, but many underlying mechanisms of the mode of action are poorly understood. We report the x-ray structure of the acetylcholine-binding protein from *Lymnaea stagnalis* with NS9283, a stoichiometry selective positive modulator that targets the $\alpha4$-$\alpha4$ interface of $\alpha4\beta2$ nicotinic acetylcholine receptors (nAChRs). Together with homology modeling, mutational data, quantum mechanical calculations, and pharmacological studies on $\alpha4\beta2$ nAChRs, the structure reveals a modulator binding mode that overlaps the $\alpha4$-$\alpha4$ interface agonist (acetylcholine)-binding site. Analysis of contacts to residues known to govern agonist binding and function suggests that modulation occurs by an agonist-like mechanism. Selectivity for $\alpha4$-$\alpha4$ over $\alpha4$-$\beta2$ interfaces is determined mainly by steric restrictions from Val-136 on the $\beta2$-subunit and favorable interactions between NS9283 and His-142 at the complementary side of $\alpha4$. In the concentration ranges where modulation is observed, its selectivity prevents NS9283 from directly activating nAChRs because activation requires coordinated action from more than one interface. However, we demonstrate that in a mutant receptor with one natural and two engineered $\alpha4$-$\alpha4$ interfaces, NS9283 is an agonist. Modulation via extracellular binding sites is well known for benzodiazepines acting at γ-aminobutyric acid type A receptors. Like NS9283, benzodiazepines increase the apparent agonist potency with a minimal effect on efficacy. The shared modulatory profile along with a binding site located in an extracellular subunit interface suggest that modulation via an agonist-like mechanism may be a common mechanism of action that potentially could apply to Cys loop receptors beyond the $\alpha4\beta2$ nAChRs.

Neuronal nicotinic acetylcholine receptors (nAChRs)[3] and γ-aminobutyric acid type A receptors ($GABA_A$Rs) are important ion channels that belong to the Cys loop family of receptors. They are expressed in the central nervous system where they contribute to excitatory and inhibitory neurotransmission, respectively (1, 2). Both receptor types are implicated as either cause or remedy in devastating diseases, including anxiety, Parkinson, and Alzheimer diseases, pain, and attention deficit hyperactivity disorder (3–5). Therefore, the development of drugs that target these receptors is a priority area for research (3, 6). Although allosteric modulators are mechanistically less well understood than agonists, they are believed to have advantages as pharmaceuticals. First and foremost, they cause less tonic activation and receptor desensitization, *i.e.* the normal temporal and spatial resolution of neuronal firing is maintained, which may result in better tolerated drugs (7, 8). Furthermore, modulator binding sites are often located in less structurally conserved regions than the agonist-binding sites, which suggest that it may be easier to obtain subtype-selective modulators (7–9).

It is becoming apparent that different modulator "phenotypes" exist, and at least some of these can be linked to distinct modulator binding sites (4, 10). A classic example of this is etomidate and benzodiazepine modulators at $GABA_A$Rs, which work through different binding sites and have very distinct modulatory profiles (11). Etomidate binds to sites in the transmembrane region of the receptor where it modulates $GABA_A$R

* This work was supported by NeuroSearch A/S and the Danish Agency for Science, Technology and Innovation, the DRA Research School at the University of Copenhagen, Denmark, the IMK Almene Fond, Denmark, and Australian National Health and Medical Research Council Grant APP1069417. J. A. O. and P. K. A. declare that at the time the described work was carried out they were employed by NeuroSearch A/S or Saniona AB, respectively. This does not alter the authors' adherence to all policies on sharing data and materials.

The atomic coordinates and structure factors (code 4NZB) have been deposited in the Protein Data Bank (http://wwpdb.org/).

[1] Supported by NeuroSearch A/S and the Danish Agency for Science, Technology and Innovation.

[2] To whom correspondence should be addressed: Faculty of Pharmacy, The University of Sydney, Sydney, New South Wales 2006, Australia. Tel.: 61-2-9036-7035; E-mail: thomas.balle@sydney.edu.au.

[3] The abbreviations used are: nAChR, nicotinic acetylcholine receptor; ACh, acetylcholine; *Ac, Aplysia californica*; AChBP, acetylcholine-binding protein; CRR, concentration response relationship; *Ls, Lymnea stagnalis*; $5\text{-}HT_3AR$, 5-hydroxytryptamine type 3A receptor; $GABA_AR$, $GABA_A$ receptor.

efficacy levels at low concentrations and directly activates at high concentrations, similarly to the barbiturate type of modulators at this receptor (12, 13). In contrast, benzodiazepines only modulate the GABA potency and are known to bind in an extracellular pocket in the receptor α-γ interface, a pocket that is structurally similar to the GABA-binding β-α-subunit pocket (6, 9).

Recently, an $\alpha4\beta2$ nAChR modulator, NS9283 (Fig. 1*A*), with a benzodiazepine-like phenotype was reported. NS9283 improves cognitive function in animal models, and it enhances the analgesic effects of the nonopioid analgesic ABT-594 (14, 15). These preclinical data provide hope that positive modulators of $\alpha4\beta2$ nAChRs may realize some of the therapeutic benefits (3, 8, 16) that were anticipated to come from agonist discovery programs (3, 17).

NS9283 is a stoichiometry selective modulator that targets the $\alpha4$-$\alpha4$ interface present in $\alpha4\beta2$ receptors composed of three $\alpha4$- and two $\beta2$-subunits (15, 18). Furthermore, mutations in the $\alpha4$-subunit have pointed to residues near the acetylcholine (ACh)-binding site to be critical for NS9283 actions (10), thereby hinting that resemblance to benzodiazepines may extend beyond pharmacological actions. Given that benzodiazepine-type modulators have proven extremely useful at $GABA_A$Rs, and modulators with similar profiles at $\alpha4\beta2$ nAChRs now turn out to be promising drug-discovery lead compounds, further investigations of these shared modulatory mechanisms may provide important insights applicable to the whole family of Cys loop receptors.

In this report, we have co-crystallized NS9283 with the ACh-binding protein from *Lymnaea stagnalis* (*Ls*-AChBP). Supported by homology modeling and mutational data on $\alpha4\beta2$ nAChRs, the results convincingly show a binding mode overlapping the ACh binding pocket in the $\alpha4$-$\alpha4$-subunit interface. Furthermore, NS9283 was observed to directly activate engineered receptors with three sites capable of binding NS9283. Collectively, the data show that although NS9283 functionally appears to be a classical positive allosteric modulator, mechanistically it works the same way as an agonist, albeit constrained to a single subunit interface at the tested concentrations.

EXPERIMENTAL PROCEDURES

Materials—NS9283 (3-(3-(pyridine-3-yl)-1,2,4-oxadiazol-5-yl)benzonitrile) was synthesized at NeuroSearch A/S. ACh (A9101), and all other chemicals were of analytical grade and purchased from Sigma unless otherwise specified.

Molecular Biology—Mutations were introduced into plasmid expression vectors coding for human $\alpha4$ and $\beta2$ nAChR subunits (19) by site-directed mutagenesis as described previously (20). Custom-designed oligonucleotides were ordered from Eurofins MWG Operon. Mutations were confirmed by sequencing (MWG Operon), and cRNA was produced using the mMessage mMachine T7 transcription kit (Ambion) according to the manufacturer's instructions.

Radioactive Ligand Binding—An *Ls*-AchBP/5-HT_3AR chimera was stably expressed in HEK293 cells (CRL-1573, American Type Culture Collection) and prepared for binding experiments as described previously (21). Briefly, cell pellets were thawed, washed in 15 ml of Tris-HCl (50 mM, pH 7.4), treated with an Ultra-Turrax homogenizer, centrifuged for 10 min at 4 °C and 25,000 relative centrifugal force, and resuspended in ice-cold Tris-HCl buffer (50 mM, pH 7.4). Affinity of NS9283 was determined by displacement of [^{3}H]epibatidine (250 μCi, NET1102250UC, PerkinElmer Life Sciences). 800 μl of tissue suspension was mixed with 100 μl of NS9283 solution in 48% ethanol and 100 μl of an ~0.3 nM [^{3}H]epibatidine solution in 48% ethanol. The specific concentration of the [^{3}H]epibatidine solution was determined by liquid scintillation counting. Binding was terminated after incubation for 1 h by filtration over GF/C glass fiber filters (Brandel Inc.) preincubated for 30 min with 0.1% polyethyleneimine. Nonspecific binding was tested by incubation with an excess of (−)-nicotine (30 μM). Filters containing protein and bound [^{3}H]epibatidine were individually incubated for at least 4 h with 3 ml of Ultima Gold (PerkinElmer Life Sciences). Radioactivity was then measured by liquid scintillation counting on a Tri-Carb counter (PerkinElmer Life Sciences), and IC_{50} values were determined by nonlinear regression using GraphPad Prism, with all points in one experiment determined in triplicate. The K_i value was determined from the average IC_{50} values of three individual experiments by the Cheng-Prusoff equation: $K_i = IC_{50}/(1 + L/K_d)$, where L is the concentration of [^{3}H]epibatidine used in the assay, and K_d is the dissociation constant for [^{3}H]epibatidine at *Ls*-AChBP (0.097 nM) as determined previously (22).

Electrophysiology—Two-electrode voltage clamp electrophysiology recordings were carried out using *Xenopus laevis* oocytes as described previously (23). Briefly, oocytes were injected with ~25 ng of cRNA with a ratio between $\alpha4$- and $\beta2$-subunit cRNAs of 4:1 or 10:1, to give $3\alpha{:}2\beta$ stoichiometry. Injected oocytes were incubated for 2–7 days at 18 °C in modified Barth's solution (90 mM NaCl, 1.0 mM KCl, 0.66 mM $NaNO_3$, 2.4 mM $NaHCO_3$, 10 mM Hepes, 2.5 mM sodium pyruvate, 0.74 mM $CaCl_2$, 0.82 mM $MgCl_2$, 100 μg/ml gentamycin, and pH adjusted to 7.5). Oocytes were placed in a custom-designed recording chamber and voltage clamped at a holding potential ranging from −40 to −80 mV using a Geneclamp 500B amplifier (Axon). Pipette resistances were 0.6–2.0 megohms in OR2 (90 mM NaCl, 2.5 mM KCl, 2.5 mM $CaCl_2$, 1.0 mM $MgCl_2$, 5.0 mM Hepes, and pH adjusted to 7.5). Fresh solutions of NS9283 and ACh were prepared on the day of measurement in OR2 and applied to the oocytes with a flow rate of 2.0 ml/min via a glass capillary. Signals were low-pass filtered at 20 Hz and digitized at 200 Hz by a Digidata 1322A (Axon) digitizer. Traces were recorded in Clampex 10.2 and subsequently analyzed in Clampfit 10.2 (Axon). Traces were baseline-subtracted, and responses to individual applications were read as peak current amplitudes. Concentration-response relationships (CRRs) were fitted in GraphPad Prism to a monophasic Hill equation constrained with a Hill slope of 1 and starting at zero. All data sets were constructed from at least five oocytes and recorded on a minimum of 2 experimental days.

Protein Expression and Crystallization—*Ls*-AChBP was expressed in *Sf*-9 cells using the Bac-to-Bac baculovirus expression system and purified by ion-exchange chromatography as described previously (24). A solution of ~ 0.2 mg/ml protein and 0.4 mM NS9283 in 0.1 M Tris, pH 8.0, 0.2 M NaCl, and 5% DMSO was equilibrated at 4 °C for 20 h, with some precipitate

forming. The solution was subsequently concentrated to an estimated protein concentration of 5 mg/ml and used immediately for crystallization experiments. Crystals were obtained by sitting drop vapor diffusion at 20 °C by mixing 1 μl of protein/ligand solution with 1 μl of crystallization solution containing 0.1 mM Tris, pH 8.0, 1.9 M $(NH_4)_2SO_4$, and 4% PEG 400. Crystals were supplemented with glycerol containing crystallization solution to a final glycerol concentration of ~25% before being mounted on cryo-loops and cooled in liquid nitrogen. Data were collected at MAX-lab in Lund, Sweden, on beamline I911-3 at 101 K using a wavelength of 1.000 Å. Images were collected as 0.3° ϕ slices on a marmosaic 225 detector.

Data Processing and Refinement—XDS (S4) was used for initial data processing and SCALA in CCP4 (25) for scaling and creation of an *R*free set from 5% of the total data. The structure of *Ls*-AChBP in complex with NS9283 was determined by molecular replacement using the PHENIX program suite (26) based on a template from Protein Data Bank code 3ZDG (chains A to E) (27) with loop C removed. The subsequent model was refined in iterative steps of manual model adjustment in COOT (28) and refinement in PHENIX. *B* factors were refined as individual isotropic values. NS9283 was built in Maestro, and geometry restraints and cif-file were generated with eLBOW in PHENIX. Noncrystallographic symmetry (NCS) restraints were used in refinement steps; however, residues within 5 Å of the modulator-binding pocket were excluded as well as residues 22–25 (loop A) and 155–163 (loop F). For statistics on data collection and refinement, see Table 1.

Molecular Modeling—Models of the extracellular domain of a dimer between two α4 nAChR subunits were created and evaluated based on the procedure described previously (20), but with the NS9283 co-crystal structure replacing the 1UW6 template and NS9283 replacing nicotine. In this way, the refined structure between NS9283 and *Ls*-AChBP was used to define the binding site region in the model. One hundred models of the dimer with NS9283 bound in the interface were prepared in MODELLER Version 9.12 (29), and the highest ranked model according to Discrete Optimized Protein Energy (DOPE) score (30) was selected. Subsequently, nonconserved residues within 5 Å of NS9283 were sampled in PRIME (31) to predict side-chain conformations while taking electrostatics of the ligand into consideration. Quantum mechanical calculations were performed on the NS9283 molecule extracted from the chain C-D interface of the *Ls*-AChBP co-crystal structure. After preparation of the modulator, the geometry was optimized using the B3LYP/6–31G* method keeping ring-connecting dihedrals frozen. Subsequently, the electrostatic potential was calculated using the B3LYP/CC-PVTZ++ functional and basis set implemented in Jaguar (version 7.9, Schrödinger, LLC). The SCF convergence criteria was set to "ultrafine."

RESULTS

The ACh-binding protein (AChBP) has been used frequently as a model for $\alpha4\beta2$ nAChRs (22, 32) to investigate interactions of agonists and antagonists with extracellular binding sites and, less frequently, modulators (33). An extracellular binding site for the $\alpha4\beta2$-positive allosteric modulator NS9283 is suggested from several datasets. Experiments with chimeric receptors link efficacy to the extracellular domain of $\alpha4\beta2$ receptors (10). Furthermore, mutation of three residues, His-142, Gln-150, and Thr-152, in the complementary α4-subunit interface, abolishes all NS9283 actions, which indicate binding in this region (10). Interestingly, these same point mutations were previously shown to affect potency of ACh for the $\alpha4$-$\alpha4$ site, which could indicate partly or fully overlapping binding sites for NS9283 and ACh (20).

Previously, NS9283 was shown to not displace or otherwise affect [^{3}H]cytosine binding at rat cortical membranes (15). To determine whether NS9283 displaces [^{3}H]epibatidine from *Ls*-AChBP, initial experiments were performed on membranes from HEK293 cells expressing an *Ls*-AChBP/5-HT_3AR chimera (22). Surprisingly, NS9283 did in fact clearly displace epibatidine with a calculated K_i of 67 μM (Fig. 1*B*), but due to precipitation at high concentrations (>300 μM), full displacement could not be obtained under the experimental conditions.

Ls-AChBP was next successfully co-crystallized in presence of an ~400 μM suspension of NS9283. The resulting crystals in the space group C2 diffracted to 2.7 Å resolution (Table 1). In the crystal structure, subunits were in the expected pentameric arrangement with three pentamers in the asymmetric unit of the crystal, each subunit consisting of a core β-sandwich structure and several important loop regions (Fig. 1, *C* and *D*) (32).

NS9283 Binds to Ls-AChBP in the ACh Binding Pocket—Following structure determination by molecular replacement and initial refinement, additional electron density was visible at all interfaces in the electron-rich aromatic box around Trp-143. This region is homologous in sequence to the ACh binding pocket in nAChRs and is also the binding site for other $\alpha4\beta2$ ligands, including nicotine, carbamoylcholine, and dihydro-β-erythroidine (10, 29, 34). NS9283 was unambiguously built into six interfaces out of the total of 15 that compose the three pentamers of the asymmetric crystallographic unit (Fig. 1, *D*–*F*). As the electron density in the remaining sites did not allow unambiguous positioning of NS9283, they were left unmodeled. For AChBP complexes with low affinity ligands, it is common that only some sites have ligands modeled, *e.g.* in some binding sites with neonicotenoids, cocaine, galanthamine, and carbamoylcholine (24, 33, 35). In the sites where NS9283 is modeled, it binds in a single well defined conformation, but the exact location varies slightly between sites (root mean square deviation = 0.4 Å) (Fig. 1*G*) as does capping of the binding site by the tip of loop C (Fig. 1*G*).

The best defined electron density for NS9283 (Fig. 1, *E* and *F*) was observed in the interface between chains B and C and is consequently used in the following analysis (deviations observed in other, largely similar, interfaces are indicated in Fig. 1*G*). The ligand mainly interacts with conserved residues on the principal side of the interface (Fig. 1*E*) as follows: (i) the pyridine ring of NS9283 stacks with Tyr-89 at a centroid-centroid distance of 4.0 Å; (ii) the oxadiazole moiety interacts with the backbone carbonyl oxygen of Trp-143 at a distance of 3.1 Å, measured to C5 of the oxadiazole; (iii) the pyridine nitrogen is within hydrogen bonding distance (2.7 Å) of Tyr-185; and (iv) the nitrogen of the nitrile is within hydrogen bonding distance (3.1 Å) of Tyr-192. On the complementary side of the interface, the N2 of the oxadiazole is located 4.0 Å away from the centroid

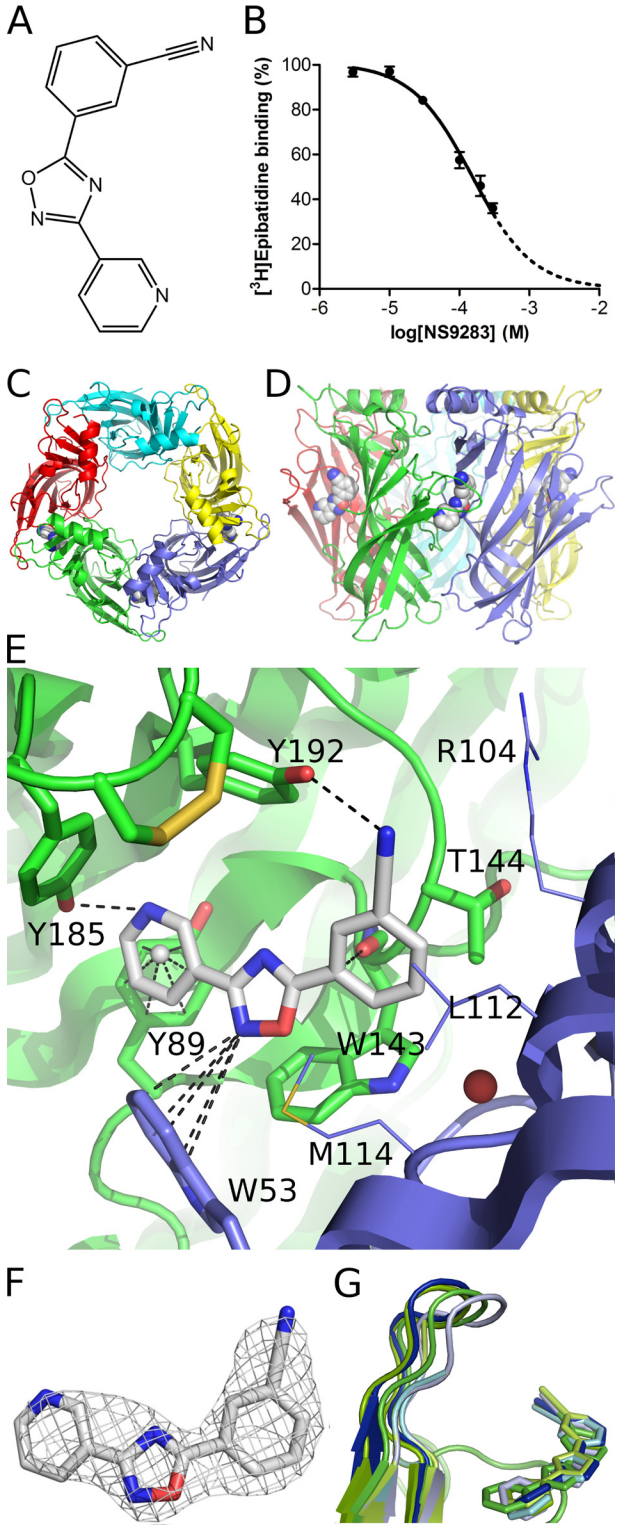

FIGURE 1. **NS9283, chemical structure, binding, and co-crystal structure with *Ls*-AChBP.** *A,* chemical structure of NS9283. *B,* [^{3}H]epibatidine displacement by NS9283 from an *Ls*-AChBP/5-HT$_{3A}$R chimera expressed in HEK293 cells. NS9283 was not soluble at concentrations exceeding 300 μM under the experimental conditions. Data were fitted to a one-site competitive binding equation giving an IC_{50} value of 67 μM ($pK_i = 4.17 \pm 0.43$ (S.D.), $n = 6$). *C,* top view of the crystal structure of *Ls*-AChBP with NS9283 determined at 2.7 Å resolution. *D,* side view of the *C* and *D* interface with NS9283 bound. NS9283 is shown as a space-filling model. *E,* binding mode of NS9283 (*gray sticks*) in the crystal structure. Residues conserved with respect to the α4-α4 interface in nAChRs are shown as *sticks* and nonconserved residues within 5 Å of NS9283 as *lines*. *Green residues* are from the principal (+) subunit, and *blue residues* are from the complementary (−) subunit. Interactions are highlighted as *dashed black lines*. The binding mode is representative of three interfaces where loop C is the most closed. The water molecule seen interacting with the complementary side of the interface is not visible from the density in all interfaces. *F,* mesh around NS9283 corresponds to a $2mF_c - DF_co$ map at a level of 1σ, showing the electron density around the ligand in the refined model. *G,* loop C adopts several distinct conformations in the interfaces with bound NS9283, which do not seem to arise from crystal packing effects. Figures were created using the PyMOL software (The PyMOL Molecular Graphics System, Version 1.5.0.4 Schrödinger, LLC).

TABLE 1
Crystallography statistics

Data collection	
Space group	C2
a, *b*, *c* (Å)	231.73, 140.38, 119.55
α, β, γ (°)	90.00, 89.98, 90.00
Reflections, overall	378,581
Reflections, unique	102,572
Resolution range (Å)	28.37–2.68 (2.82–2.68)[a]
I/σ_I	8.9 (2.0)
Completeness (%)	98.1 (87.6)
Multiplicity	3.6 (2.3)
R_{merge} (%)[b]	7.2 (37.9)
Mosaicity (°)	0.19
Pentamers/AU[c]	3
Refinement	
No. of residues	
Protein	2963
NS9283	6
Water	336
R(work) (%)[d]	21.0
R(free) (%)[d]	24.6
r.m.s.d.[e] bonds (Å)	0.014
r.m.s.d. bonds (°)	1.3
Ramachandran outliers (%)[f]	0.1
Ramachandran favored (%)[f]	97.3
Average *B* (Å^2)	
Protein	50
NS9283	68
Water	40

[a] Numbers in parentheses correspond to the outer resolution bin.
[b] A measure of agreement among multiple measurements of the same reflections. R_{merge} is calculated as follows: $I_i(hkl)$ is the intensity of an individual measurement of the reflection with Miller indices *hkl*, and $I(hkl)$ is the intensity from multiple observations $R_{merge} = \sum_{hkl}\sum_i|I_i(hkl) - I(hkl)|/\sum_{hkl}\sum_i|I_i(hkl)|$.
[c] AU means asymmetric unit of the crystal.
[d] $R(work) = \sum_{hkl}|F_{obs} - F_{calc}|/\sum_{hkl}|F_{obs}|$, where F_{obs} and F_{calc} are the observed and calculated structure factor amplitudes, respectively. The free *R* factor, *R*(free), is computed in the same manner as *R*(work), but using only a small set (5%) of randomly chosen reflections not used in the refinement of the model.
[e] r.m.s.d. means root mean square deviation.
[f] The Ramachandran plot was calculated using PHENIX. The outliers are at the borderline of allowed regions.

of the conserved Trp-53, and modulator binding is further supported by van der Waals interactions to Arg-104, Leu-112, and Met-114. Among the observed interactions, the contact between the oxadiazole and the Trp-143 carbonyl oxygen appeared unusual and was therefore further investigated by quantum mechanical calculations to map the molecular surface properties of NS9283. This revealed that the area around C5 of the oxadiazole ring and C3 of the benzonitrile is electron-deficient as evident from the positive electrostatic potential (Fig. 2), suggesting that favorable interaction to the carbonyl oxygen is contributing to binding.

NS9283 Forms an Inter-subunit Bridge in α4-α4 Interfaces—The principal side residues forming direct contacts to NS9283 are fully conserved between *Ls*-AChBP and the α4 nAChR subunit. However, when comparing contact residues on the complementary subunit interface of *Ls*-AChBP with those in the classical agonist binding pockets of α4-β2 or α4-α4 interfaces, only Trp-53 corresponding to Trp-88 and Trp-82 in α4 and β2,

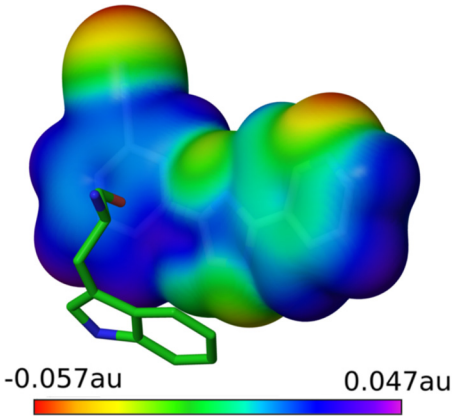

FIGURE 2. **Electrostatic potential map of NS9283.** Trp-143 from *Ls*-AChBP is displayed along with the map and shows the carbonyl oxygen of Trp-143 pointing toward an area with a positive electrostatic potential (*blue surface*). Quantum mechanical calculations (B3LYP/CC-PVTZ++//B3LYP/6–31G*) were performed in Jaguar (version 7.9, Schrödinger, LLC, New York). *au*, atomic units.

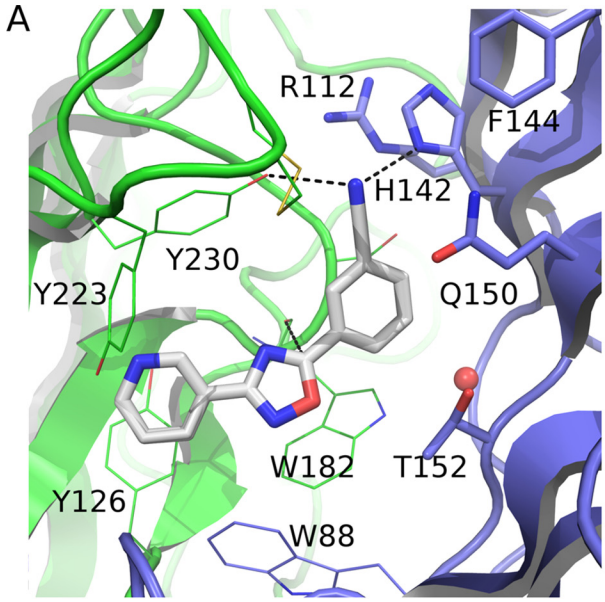

B

Principal (+) side

α4	(124)VLYNN	(180)GSWTY	(222)KYECCAEIYP
β2	(118)VLYNN	(174)RSWTY	(216)-PDDS-T-YV
AChBP	(87)AAYN-	(141)GSWTH	(184)TYSCCPEAYE

Complementary (-) side

α4	(86)NVWVK	(110)SIRIP	(139)TKAHLFHDGRVQWTP
β2	(80)NVWLT	(104)KVRLP	(133)SNAVVSYDGSIFWLP
AChBP	(51)VFWQQ	(73)QVSVP	(101)QLARVVSDGEVLYMP

FIGURE 3. **Homology model showing NS9283 binding at the α4-α4 interface.** *A,* nonconserved residues (α4β2 *versus Ls*-AChBP) are shown as *sticks*, and conserved residues are shown as *lines*. Residues on the principal α4(+) and complementary α4(−) side are colored *green* and *blue*, respectively. *B,* alignment of human nAChR subunits α4 and β2 and *Ls*-AChBP based on a multiple alignment from Ref. 32.

respectively, are conserved. The remaining contact residues, Arg-104 (which only exposes its hydrophobic carbon chain to the binding site), Leu-112, and Met-114 make the complementary binding interface hydrophobic in nature, and thus it best resembles the β2(−) interface with Val-136, Phe-144, and Leu-146 in corresponding positions (22, 32). When considering the α4-α4 interface, where the corresponding residues His-142, Gln-150, and Thr-152 are hydrophilic in nature (20), the use of *Ls*-AChBP as a model system to predict important ligand-receptor interactions is complex.

Therefore, as NS9283 binds in the α4-α4 interface of α4β2 nAChRs, a homology model of this interface was constructed using the NS9283 x-ray structure as one of the templates. Particular focus was placed on defining the binding site region, and a procedure similar to that previously reported by Harpsøe *et al.* (20) was used. This model (Fig. 3) is highly comparable with the *Ls*-AChBP on the principal side with interactions similar to those in the B-C interface of the x-ray structure; however, it also suggests potential interactions of NS9283 with nonconserved residues on the complementary side of the α4-subunit. In particular, hydrogen bonding is predicted from His-142 to the nitrile group of NS9283. This interaction appears to involve peripheral residues Arg-112 and Phe-144, stacking with the histidine and shielding the polar histidine and arginine from the surrounding solvent. In summary, the model supports an NS9283-mediated inter-subunit bridge that may be stronger in an α4-α4 interface than in *Ls*-AChBP.

Mutations Validate NS9283 Contacts—To investigate the observed binding mode of NS9283, we performed a mutational scan of residues on the complementary side of the α4-α4 interface that were predicted, based on the x-ray structure, to be in proximity of the compound. By only introducing mutations on the α4 complementary interface, the α4-β2 interfaces are left intact for ACh binding. The mutant constructs were expressed with wild-type (WT) β2 in *Xenopus* oocytes in 3α:2β stoichiometries, and modulatory effects of NS9283 were measured by two-electrode voltage clamp electrophysiology. NS9283 concentrations from 0.01 to 31.6 μM were co-applied with 10 μM ACh, and the EC_{50} value of the resulting CRR was used as the measure of modulatory potency. In total, 15 mutant constructs were tested, and all were responsive to applications of ACh. Current waveforms and current levels were, except for Trp-88 mutations (discussed below), comparable with those of WT receptors (Fig. 4 and Table 2).

As mentioned, an α4 complementary side mutant, where three residues were changed to the corresponding residues in β2, H142V, Q150F, and T152L, obliterates all NS9283 activity (10). When mutated individually, a similar effect was seen with the H142V mutant, whereas the Q150F and T152L mutations resulted in decreased functional potency by a factor of 2 and 3, respectively (Table 2 and Fig. 5*A*). To investigate whether the detrimental effect of H142V was due to lack of interaction with the histidine or rather a disruptive steric effect of the more bulky valine, an alanine was next tested in this position. At H142A mutated receptors, NS9283 showed modulatory efficacy albeit with an ~10-fold decreased EC_{50} value (Fig. 5, *B* and *C*), which indicates that a combination of both above-mentioned explanations causes the obliteration of efficacy at the H142V construct.

In the *Ls*-AChBP structure, the Trp-53 residue was seen as the only conserved interaction from NS9283 to the complementary interface (Trp-88 in α4). To investigate the impor-

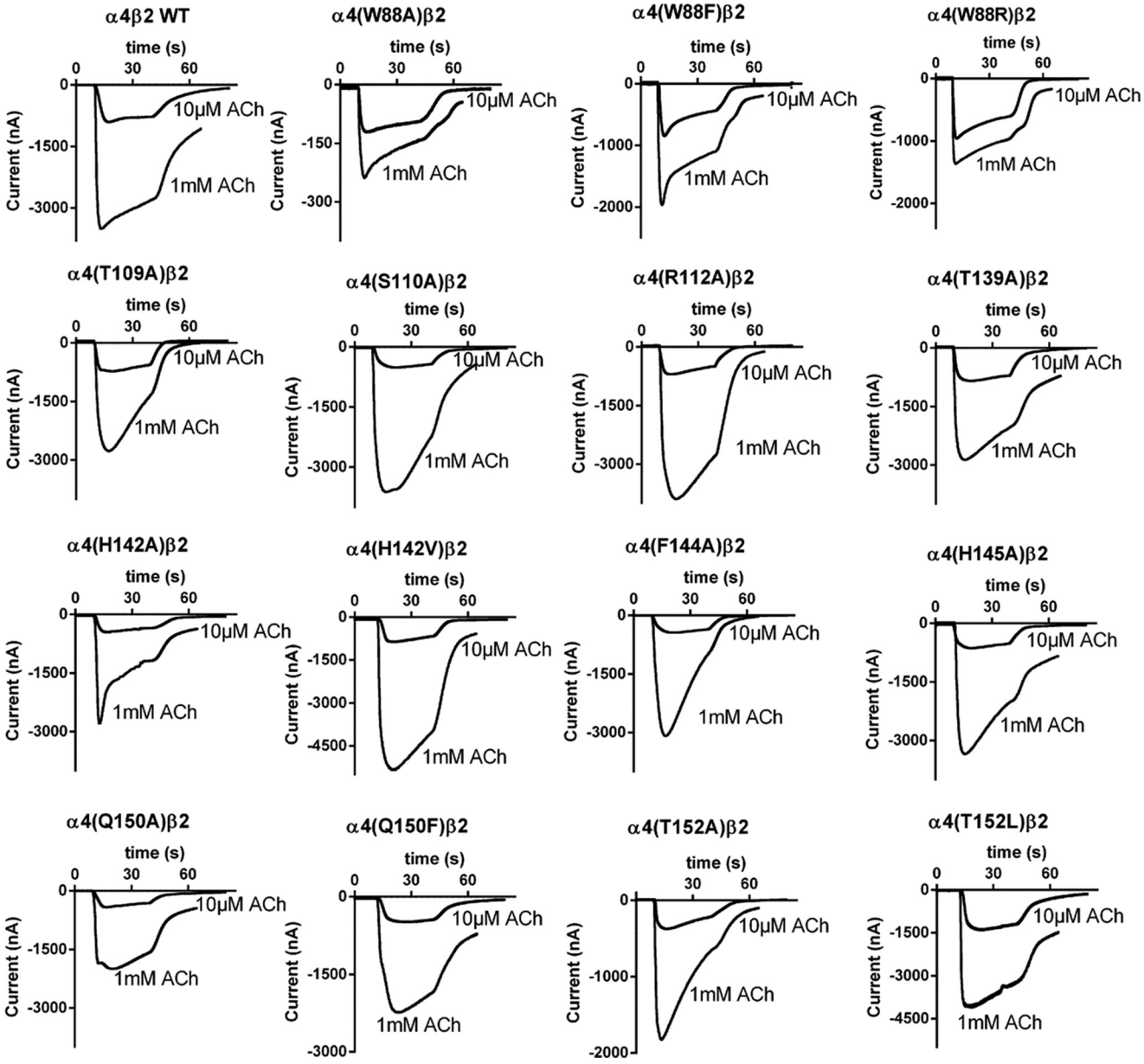

FIGURE 4. **Representative traces from two-electrode voltage clamp experiments on $\alpha4\beta2$ nAChRs and mutants thereof expressed in *X. laevis* oocytes.** ACh-evoked responses in WT and point-mutated $\alpha4\beta2$ receptors were recorded in *X. laevis* oocytes as described in Table 2 legend. For all mutants, representative traces are shown from applications of 10 μM and 1 mM ACh to the same oocyte. All mutants respond to ACh in a concentration-dependent manner and with current waveforms resembling WT receptors (*upper left corner*) as inspected visually. The ratio between ACh-evoked currents at 1 mM and 10 μM concentrations, $I_{1\ mM\ ACh}$ and $II_{10\ \mu M\ ACh}$, can be seen as an indicator of whether a particular mutation results in a functional $\alpha4$-$\alpha4$ site with respect to ACh activation. ($I_{1\ mM\ ACh}$)/($I_{10\ \mu M\ ACh}$) ratios are seen in Table 2. Note that the W88A, W88F, and W88R mutants give significantly lowered ratios compared with WT indicating a compromised site. These mutants are discussed in the text.

tance of Trp-88 for NS9283 activity, three point mutants W88A, W88F, and W88R were tested. W88R resulted in receptors that were unresponsive to NS9283, whereas W88A and W88F resulted in greatly reduced modulator potency (Fig. 5, *B* and *C*). It is noteworthy that these three mutations, in contrast to the other mutations tested here, also clearly affect the ability of ACh to activate the receptor through the $\alpha4$-$\alpha4$-binding site (Fig. 4 and Table 3). Full ACh CRRs with the W88R and W88F mutants were similar to previous data observed for the W88A mutant (36), but the mutational effects appear more pronounced. For both mutants, ACh activation via the $\alpha4$-$\beta2$ sites is uncompromised as evidenced by the EC_{50} values close to 1 μM (Table 3). In the W88F mutant, ACh activation through the low affinity $\alpha4$-$\alpha4$ site is clearly visible although with an ~30-fold decreased EC_{50} value; however, in the W88R mutant $\alpha4$-$\alpha4$ site activation is severely compromised. For the Trp-88 mutants, the high affinity component of the biphasic Hill curve fit accounts for a larger proportion compared with the WT receptor (Table 3), which is to be expected because the mutations partly or completely disrupt ACh-evoked receptor activation through the $\alpha4$-$\alpha4$ site. Thus, Trp-88 appears to be central for ACh actions in the $\alpha4$-$\alpha4$ site, and the relative effects of these mutations W88R > W88F > W88A match the order observed for NS9283. This is expected given the

binding mode of NS9283 and suggests that NS9283 has direct interaction with Trp-88, as was clearly indicated by the AChBP binding mode.

TABLE 2

NS9283 modulation of ACh-evoked responses at wild-type and mutant nAChRs using *X. laevis* oocyte two-electrode voltage clamp electrophysiology

Oocytes were injected with WT or point-mutated α4 subunits mixed with WT β2 subunits in a 10:1 cRNA ratio to yield receptors in the $(\alpha4^{Mutant})_3(\beta2)_2$ stoichiometry. $(I_{1\ mM\ ACh})/(I_{10\ \mu M\ ACh})$ ratios were obtained as described in the Fig. 4 legend and are presented ± S.D. values. * indicates a statistically significant difference from WT (one-way ANOVA, $\alpha = 0.01$). CRRs for NS9283 were obtained by co-application with an ~EC_{10} concentration of ACh (10 μM) as described in Olsen *et al.* (10). Data were fitted to the empirical Hill equation using nonlinear regression with a fixed bottom of 0 and a Hill slope of 1 and are presented with 95% confidence intervals as EC_{50} in micromolars and maximal efficacy E_{max} in percent from the indicated number of experiments. NA indicates no NS9283 modulation was noted.

Mutation	$(I_{1\ mM\ ACh})/(I_{10\ \mu M\ ACh})$	NS9283 EC_{50}	NS9283 E_{max}	*n*
α4		μM	%	
None (WT)[a]	4.6 (±1.1)	3.4 (1.5–7.9)	680 (530–830)	6
W88A	1.6* (±0.2)	110 (6.1–2100)[b]	560 (0.0–1890)[b]	6
W88F	1.9* (±0.3)	51 (12–220)	410 (6.4–820)	7
W88R	1.8* (±0.5)	NA	NA	9
T109A	5.1 (±1.2)	2.7 (1.8–4.1)	580 (520–650)	6
S110A	9.2* (±1.5)	3.9 (1.9–8.0)	1700 (1300–2100)	4
R112A	5.6 (±1.0)	40 (17–90)	240 (110–370)	7
T139A	4.2 (±0.9)	5.1 (2.6–10)	400 (310–490)	8
H142A	8.1* (±1.5)	36 (16–78)	780 (420–1100)	6
H142V	6.8 (± 2.2)	NA	NA	14
F144A	7.5* (±1.5)	22 (10–50)	900 (550–1300)	8
H145A	5.9 (±2.4)	1.6 (0.89–2.7)	430 (380–480)	4
Q150A	4.2 (±1.6)	5.7 (2.1–16)	469 (310–630)	5
Q150F	3.5 (±1.4)	6.9 (3.5–14)	570 (430–700)	12
T152A	5.0 (±1.3)	40 (16–99)	210 (130–290)	6
T152L	4.3 (±0.9)	11 (6.1–22)	360 (270–440)	9

[a] Data are from Ref. 10.
[b] 95% confidence interval is wide at this mutant due to low NS9283 efficacy at maximally applied concentrations.

An alanine scan of further residues clustered around the binding pocket of NS9283 revealed that Arg-112 and Phe-144 also contribute to NS9283 potency in good agreement with the predicted roles of these amino acids in the homology model (Fig. 5, *B* and *C*). In contrast, alanine mutations in Thr-109, Ser-110, Thr-139, and His-145 did not result in EC_{50} values of NS9283 significantly different from those at WT receptors.

NS9283 Activates Receptors with More Than One Compatible Binding Site—Because the results show a binding mode of NS9283 at the α4-α4 interface overlapping that of ACh and with interactions to residues known to interact with agonists, we hypothesized that NS9283 might be able to directly activate receptors containing more than one NS9283-binding site. To investigate this, a previously described point mutated β2-subunit was expressed in combination with α4 (20). Essentially, this β2 mutant has the reverse mutations of the above described α4 triple mutant (V136H, F144Q, and L146T), thereby giving a receptor in 3α:2β stoichiometry with two pseudo α4-α4 sites besides the native α4-α4 binding site. Although the pseudo α4-α4 sites are obviously not native α4-α4 sites, *e.g.* Phe-144 is missing, the mutations replace the valine found to be incompatible with NS9283 function and introduce the important histidine in its place.

When comparing the effect of NS9283 applications in absence of ACh on WT and α4β2(V136H, F144Q, and L146T) receptors, a clear difference is noted (Fig. 6, *A* and *B*). At WT receptors, no response was seen, whereas at the mutant receptor, NS9283 acted as an agonist with a concentration-depen-

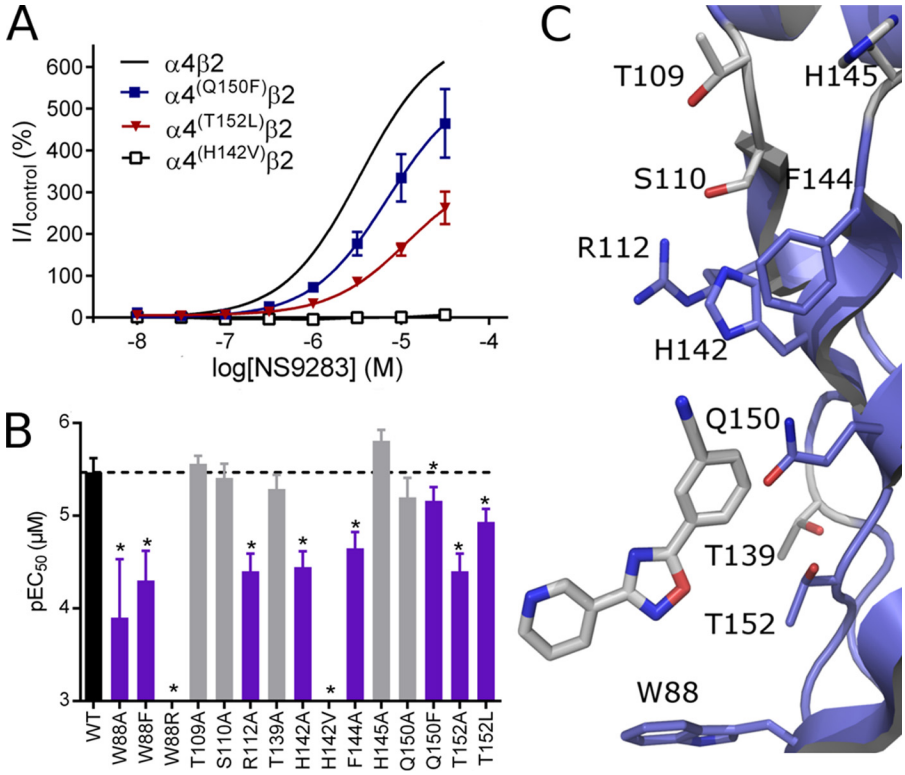

FIGURE 5. **Mutations on the complementary side of the α4-α4 interface affecting NS9283 modulatory potency.** *A,* CRRs of NS9283 modulation of WT and point-mutated α4β2 receptors were recorded in *X. laevis* oocytes as described in Table 2 legend. *B,* pEC_{50} values of NS9283 modulation at WT (*black*) and point-mutated α4β2 nAChRs (Table 2). For ease of reading, the *dotted black line* denotes the WT potency against which all *bars* are compared. Data bars for amino acids marked with * and colored *purple* were significantly different from WT (one-way analysis of variance, $\alpha = 0.01$), and data bars marked in *gray* were not. *C,* residues for which the mutation resulted in statistically significant loss of potency are shown as *sticks* and the remaining as *lines* in the α4-α4 homology model.

TABLE 3

ACh CRRs of $\alpha4^{Trp\text{-}88}$ mutants using *X. laevis* oocyte two-electrode voltage clamp electrophysiology

ACh-evoked responses in point-mutated $(\alpha4^{Mutant})_3(\beta2)_2$ receptors were recorded in *X. laevis* oocytes as described in Table 2 legend. Data were fitted to a biphasic Hill equation using nonlinear regression with a fixed bottom of 0 and a Hill slope of 1 and are presented with 95% confidence intervals as EC_{50_1} in μM, EC_{50_2} in mM, and the fraction of the high affinity component from the indicated number of experiments. Data for the WT $\alpha4\beta2$ receptor are from Harpsøe *et al*. (20), whereas data for the $\alpha4^{(W88A)}\beta2$ receptor are from Olsen *et al.* (36).

Receptor	EC_{50_1}	EC_{50_2}	Fraction	*n*
	μM	mM		
$\alpha4\beta2$	0.95	0.083	0.2	
$\alpha4^{(W88A)}\beta2$	0.87	0.150	0.7	
$\alpha4^{(W88F)}\beta2$	1.5 (1.0–2.3)	1.9 (1.0–3.7)	0.6 (0.5–0.6)	9–10
$\alpha4^{(W88R)}\beta2$	0.96 (0.65–1.4)	11 (6.0–22)	0.6 (0.5–0.6)	3–8

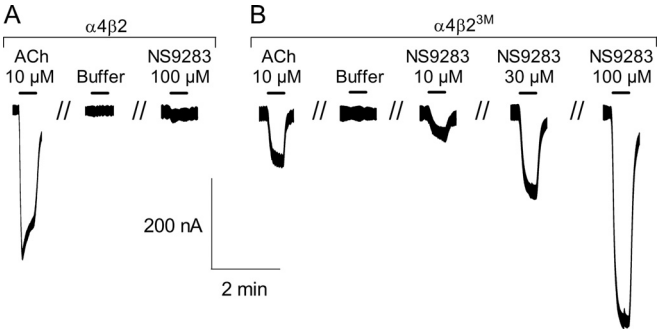

FIGURE 6. **Agonist activity of NS9283 at mutant $\alpha4\beta2^{(3M)}$ nAChR receptors.** Representative traces of ACh- and NS9283-evoked currents in WT (*A*) and $\alpha4\beta2^{(3M)}$ (*B*) receptors. *3M* signifies the mutations V136H, F144Q, and L146T. *A* and *B* are on the same scale. // denotes a washout period of more than 2 min.

dent response. These results show that NS9283, in agreement with the observed agonist-like interactions in the x-ray structure, is capable of activating $\alpha4\beta2$ receptors when these have more than one binding site with $\alpha4$-$\alpha4$ characteristics.

DISCUSSION

The aim of this study was to investigate the binding site and mode of action of the positive allosteric modulator NS9283 to further our understanding of how modulators interact with their target proteins. In a previous study (10), it was shown that the action of NS9283 is obliterated after mutation of three amino acids located in the ACh binding pocket of the $\alpha4$-$\alpha4$ nAChR interface. To explore the possibility that NS9283 could bind in close conjunction or even partly or fully inside the ACh binding pocket itself, we initially investigated displacement of [^{3}H]epibatidine binding from *Ls*-AChBP. *Ls*-AChBP was chosen because, contrary to other AChBPs, it contains all the five aromatic binding pocket residues that are fully conserved in nAChRs (36). Importantly, NS9283 was found to displace epibatidine, albeit with a low inhibition constant (K_i of ~67 μM) compared with its functional potency at $\alpha4\beta2$ receptors (EC_{50} = 3.4 μM). With this in mind, crystallization experiments with purified *Ls*-AChBP were set up with the highest concentrations of NS9283 possible, and this resulted in a successful crystallized protein with the modulator bound.

In the crystal structure of *Ls*-AChBP with NS9283, we observe a binding mode where NS9283 interacts with residues known to be important for agonist action. Key interactions are observed with residues conserved between *Ls*-AChBP and an $\alpha4$-$\alpha4$ interface. The pyridine ring stacks with Tyr-89, which also forms close contacts, *e.g.* to nicotine and carbamoylcholine in their respective structures. The oxadiazole ring of NS9283 interacts with the carbonyl group of Trp-143 at a distance of 2.9 Å. The short distance to Trp-143, which acts as a hydrogen bond acceptor, *e.g.* to the *N*-methylpyrrolidine part of nicotine (24), can be explained by electrostatic interactions, as the electron withdrawing properties of the nitrile effectively de-shields C5 of the oxadiazole and C3 of the benzonitrile, leaving a partial positive charge to interact with the lone pairs of the carbonyl oxygen. This is likely important in light of NS9283 not being able to form a cation-π interaction to Trp-143 like nicotine (37).

On the complementary side of the interface, the crystal structure reveals close contact (4 Å) from *N*2 of the oxadiazole ring of NS9283 to the centroid of Trp-53, which may appear counter-intuitive. However, interactions between lone pairs and centroids of aromatic rings have been confirmed to be favorable by quantum mechanical calculations and have been observed in several x-ray structures (38, 39).

Besides the key interactions, numerous van der Waals interactions are observed to residues on the complementary side that are not conserved residues, and their importance is therefore less obvious. To evaluate interactions between NS9283 and the complementary side of an $\alpha4$-$\alpha4$ interface, two approaches were pursued as follows: 1) a homology model based on the crystal structure obtained here was built, and 2) potentially important amino acids identified by the model were investigated by functional studies on point mutated $\alpha4$ constructs. Based on the model and *Ls*-AChBP structure, the $\alpha4$ residues Trp-88, Arg-112, His-142, Phe-144, Gln-150, and Thr-152 were all shown to interact with NS9283, and in fact, point mutations of all these amino acids affected the NS9283 modulatory potency. Other $\alpha4$ residues, Thr-109, Ser-110, Thr-139, and His-145, located in or around the binding pocket and are not expected to interact with the modulator, were confirmed to be functionally silent with respect to NS9283 potency.

Of the residues on the complementary side identified to be important in the mutational studies, only Trp-88 is conserved in *Ls*-AChBP (Trp-53), where it is located ~4 Å from the oxadiazole ring of NS9283. Mutating Trp-88 to an alanine or phenylalanine impairs NS9283 modulatory potency by an order of magnitude, indicating that tryptophan-specific interactions are important. Substituting Trp-88 with the longer arginine abolished modulation, as expected for steric reasons based on the crystal structure with *Ls*-AChBP. It is noteworthy here that ACh activation through the $\alpha4$-$\alpha4$ interface is similarly affected (Fig. 4 and Table 3) by these mutations. This give emphasis to the observation that the binding mode of NS9283 mimic those of agonists.

Of the important residues *not* conserved in *Ls*-AChBP, His-142 was especially interesting as NS9283 potency was reduced upon mutation to alanine and abolished by mutation to valine. Because a valine is present in the corresponding $\beta2$-subunit position, this single amino acid is therefore sufficient for and likely the primary determinant of the $\alpha4$-$\alpha4$ *versus* $\alpha4$-$\beta2$ interface selectivity of NS9283. In fact, the corresponding residue in $\alpha2$ is likewise a histidine, but is a leucine in $\alpha3$, consistent with

the notion that this residue position is a critical determinant of modulator selectivity given that NS9283 works on α2- and α4- but not α3-containing receptors (15). That mutation of His-142 to a valine *versus* alanine should be so unfavorable may seem surprising but can be rationalized based on the binding mode of NS9283 in *Ls*-AChBP and the homology model. A branched amino acid such as valine is, for steric reasons, not compatible with binding of NS9283. Next, the homology model suggests that the histidine side chain itself interacts with NS9283 and is in close proximity to the functionally important charged Arg-112 and Phe-144. Based on the homology model and supported by mutations, Arg-112, His-142, and Phe-144 therefore contribute significantly to anchoring the ligand to the complementary interface, which may explain the functional effect of mutation to alanine of these residues.

Although NS9283 does not structurally resemble known agonists, it does, as mentioned, show α4-α4 interface contacts resembling contacts formed by agonists. This apparent agonist-like binding mode of NS9283 leads to the question of why it has no agonist activity on its own. The most logical explanation is linked to the selectivity of the compound. As discussed above, the presence of a histidine *versus* a valine residue at the complementary interface creates a high selectivity for α4-α4 *versus* α4-β2 interfaces. Therefore, at the tested concentrations, NS9283 will only bind in one interface in a WT α4β2 receptor, which is unlikely to gate the ion channel efficiently. To investigate this hypothesis further, we utilized the α4β2(V136H, F144Q, and L146T) receptor as a surrogate for a receptor containing three α4-α4 interfaces. In this mutant β2 construct, three key complementary interface amino acids were point mutated to those of α4 (20). Expressed in 3α:2β stoichiometry, the α4β2(V136H, F144Q, and L146T) receptor effectively has one "real" and two "pseudo" α4-α4 interfaces. When tested at this receptor, NS9283 did in fact have direct agonist activity, and upon visual inspection, the evoked current waveforms resembled those of ACh (Fig. 5, *A* and *B*). The observed direct agonist activity of NS9283 underscores the observations from the crystal structure and homology model, showing the ligand to interact with the receptor in a manner resembling that of an agonist.

The collective observations on the actions and binding mode of NS9283 have some interesting implications for our understanding of how this type of modulator works. Pharmacologically, NS9283 increases apparent ACh potency with no effect on the maximal efficacy obtainable. Based on this, NS9283 was originally described as an allosteric modulator with close functional resemblance to the benzodiazepines (10, 15, 18). However, the binding to *Ls*-AChBP, the molecular interactions observed in the crystal structure, the mutational studies, and the observation that NS9283 acts as an agonist on a receptor with three compatible interfacial binding sites show that NS9283 occupies the orthosteric binding site at the α4-α4 interface and modulates via an agonist-like mechanism.

Results from the homomeric α7 nAChRs show that occupancy of two binding interfaces are required for channels to respond efficiently to ACh, although occupancy of three interfaces are required for channels to respond with maximal efficacy (39). In accordance with this, ACh activation of α4β2 receptors via the two α4-β2 sites and the α4-α4 site leads to greater current levels than activation via the α4-β2 sites alone (20). An agonist with preference for a single interface would not efficiently activate receptors to a degree observable in *Xenopus* oocytes, but together with submaximal concentrations of ACh, it would induce an increased response similar to that of a higher dose of ACh. Mechanistically, it would therefore act as an agonist, but functionally, it would behave similarly to what is described as a positive allosteric modulator.

Given that NS9283 binds in a genuine orthosteric agonist-binding site, it cannot be termed an allosteric modulator because an allosteric modulator is defined as a compound that "combines with a distinct (allosteric or allotopic) site on the receptor macromolecule" (40). Thus, nomenclature is needed for a term describing modulation via an orthosteric site by an agonist-like mechanism to help distinguish compounds such as NS9283 from true allosteric modulators that act through distinct sites. Unfortunately, the nomenclature recommendations from the "International Union of Pharmacology Committee on Receptor Nomenclature and Drug Classification" in their current form do not appear to contain a term that fully covers such a molecule (40).

On nAChRs, the described type of modulation may adhere to other modulators, including galanthamine and morantel, which all enhance potency through what is thought to be extracellular binding sites (16, 33, 41). Similarly, benzodiazepines acting on $GABA_A$Rs also produce potentiation of GABA-evoked currents without an increase in maximum efficacy. Their binding site also resides in the extracellular domain, and they form contacts across the binding interface to residues corresponding to those responsible for GABA binding in the GABA-binding site (42). The similarities in functional profiles and ligand-receptor contacts suggest that the concept may in fact also apply to benzodiazepines.

CONCLUSION

From a therapeutic perspective, positive modulators of nAChRs are of significant pharmaceutical interest. To date, only a few modulators of α4β2 receptors have been reported, and NS9283 is arguably the most promising as a drug discovery lead molecule. This study reports an x-ray structure with NS9283 bound to *Ls*-AChBP in excellent agreement with a comprehensive set of mutational data. Collectively, the data show that NS9283 binds in the α4-α4 interface in $(\alpha4)_3(\beta2)_2$ receptors where it occupies the binding site for ACh and forms contacts to residues known to be important determinants for agonist binding and function. This suggests that the mode of action of NS9283 is that of an agonist selective for a single subunit interface that is supported by data showing that NS9283 can directly activate receptors engineered to contain three compatible binding sites.

As mentioned in the Introduction, different phenotypes of allosteric modulators exist for Cys loop receptors, and their precise mode of action appears linked to the binding site they occupy. This study greatly aids in understanding the molecular actions of compounds that bind and behave like NS9283. Interestingly, an implication of this is that insights from structure-activity studies of agonists can be used in further drug discovery

efforts for new positive modulators. Hence, this can provide a basis for rational development of new drugs for nAChRs as well as other members of the Cys loop receptor family.

Acknowledgments—We thank Professor Arthur Christopoulos for valuable discussions on use of nomenclature. We also thank Professor Dr. Titia K. Sixma for providing the Ls-AChBP construct and the MAX-lab, Lund, Sweden, for providing beamtime and support during data collection.

REFERENCES

1. Lester, H. A., Dibas, M. I., Dahan, D. S., Leite, J. F., and Dougherty, D. A. (2004) Cys loop receptors: new twists and turns. *Trends Neurosci.* **27,** 329–336
2. Miller, P. S., and Smart, T. G. (2010) Binding, activation and modulation of Cys loop receptors. *Trends Pharmacol. Sci.* **31,** 161–174
3. Taly, A., Corringer, P. J., Guedin, D., Lestage, P., and Changeux, J. P. (2009) Nicotinic receptors: allosteric transitions and therapeutic targets in the nervous system. *Nat. Rev. Drug Discov.* **8,** 733–750
4. Hogg, R. C., and Bertrand, D. (2004) Nicotinic acetylcholine receptors as drug targets. *Curr. Drug Targets CNS Neurol. Disord.* **3,** 123–130
5. Gotti, C., Zoli, M., and Clementi, F. (2006) Brain nicotinic acetylcholine receptors: native subtypes and their relevance. *Trends Pharmacol. Sci.* **27,** 482–491
6. Rudolph, U., and Knoflach, F. (2011) Beyond classical benzodiazepines: novel therapeutic potential of $GABA_A$ receptor subtypes. *Nat. Rev. Drug Discov.* **10,** 685–697
7. Bertrand, D., and Gopalakrishnan, M. (2007) Allosteric modulation of nicotinic acetylcholine receptors. *Biochem. Pharmacol.* **74,** 1155–1163
8. Williams, D. K., Wang, J., and Papke, R. L. (2011) Positive allosteric modulators as an approach to nicotinic acetylcholine receptor-targeted therapeutics: advantages and limitations. *Biochem. Pharmacol.* **82,** 915–930
9. Sigel, E., and Steinmann, M. E. (2012) Structure, function, and modulation of $GABA_A$ receptors. *J. Biol. Chem.* **287,** 40224–40231
10. Olsen, J. A., Kastrup, J. S., Peters, D., Gajhede, M., Balle, T., and Ahring, P. K. (2013) Two distinct allosteric binding sites at $\alpha4\beta2$ nicotinic acetylcholine receptors revealed by NS206 and NS9283 give unique insights to binding activity-associated linkage at Cys loop receptors. *J. Biol. Chem.* **288,** 35997–36006
11. Twyman, R. E., Rogers, C. J., and Macdonald, R. L. (1989) Differential regulation of γ-aminobutyric acid receptor channels by diazepam and phenobarbital. *Ann. Neurol.* **25,** 213–220
12. Li, G. D., Chiara, D. C., Sawyer, G. W., Husain, S. S., Olsen, R. W., and Cohen, J. B. (2006) Identification of a GABAA receptor anesthetic binding site at subunit interfaces by photolabeling with an etomidate analog. *J. Neurosci.* **26,** 11599–11605
13. Loscher, W., and Rogawski, M. A. (2012) How theories evolved concerning the mechanism of action of barbiturates. *Epilepsia* **53,** 12–25
14. Lee, C. H., Zhu, C., Malysz, J., Campbell, T., Shaughnessy, T., Honore, P., Polakowski, J., and Gopalakrishnan, M. (2011) $\alpha4\beta2$ neuronal nicotinic receptor-positive allosteric modulation: an approach for improving the therapeutic index of $\alpha4\beta2$ nAChR agonists in pain. *Biochem. Pharmacol.* **82,** 959–966
15. Timmermann, D. B., Sandager-Nielsen, K., Dyhring, T., Smith, M., Jacobsen, A. M., Nielsen, E. Ø., Grunnet, M., Christensen, J. K., Peters, D., Kohlhaas, K., Olsen, G. M., and Ahring, P. K. (2012) Augmentation of cognitive function by NS9283, a stoichiometry-dependent positive allosteric modulator of $\alpha2$- and $\alpha4$-containing nicotinic acetylcholine receptors. *Br. J. Pharmacol.* **167,** 164–182
16. Pandya, A., and Yakel, J. L. (2011) Allosteric modulators of the $\alpha4\beta2$ subtype of neuronal nicotinic acetylcholine receptors. *Biochem. Pharmacol.* **82,** 952–958
17. D'hoedt, D., and Bertrand, D. (2009) Nicotinic acetylcholine receptors: an overview on drug discovery. *Expert Opin. Ther. Targets* **13,** 395–411
18. Grupe, M., Jensen, A. A., Ahring, P. K., Christensen, J. K., and Grunnet, M. (2013) Unravelling the mechanism of action of NS9283, a positive allosteric modulator of $(\alpha4)3(\beta2)2$ nicotinic ACh receptors. *Br. J. Pharmacol.* **168,** 2000–2010
19. Timmermann, D. B., Grønlien, J. H., Kohlhaas, K. L., Nielsen, E. Ø., Dam, E., Jørgensen, T. D., Ahring, P. K., Peters, D., Holst, D., Christensen, J. K., Chrsitensen, J. K., Malysz, J., Briggs, C. A., Gopalakrishnan, M., and Olsen, G. M. (2007) An allosteric modulator of the $\alpha7$ nicotinic acetylcholine receptor possessing cognition-enhancing properties *in vivo*. *J. Pharmacol. Exp. Ther.* **323,** 294–307
20. Harpsøe, K., Ahring, P. K., Christensen, J. K., Jensen, M. L., Peters, D., and Balle, T. (2011) Unraveling the high- and low-sensitivity agonist responses of nicotinic acetylcholine receptors. *J. Neurosci.* **31,** 10759–10766
21. Nielsen, S. F., Nielsen, E. O., Olsen, G. M., Liljefors, T., and Peters, D. (2000) Novel potent ligands for the central nicotinic acetylcholine receptor: synthesis, receptor binding, and 3D-QSAR analysis. *J. Med. Chem.* **43,** 2217–2226
22. Rohde, L. A., Ahring, P. K., Jensen, M. L., Nielsen, E. Ø., Peters, D., Helgstrand, C., Krintel, C., Harpsøe, K., Gajhede, M., Kastrup, J. S., and Balle, T. (2012) Intersubunit bridge formation governs agonist efficacy at nicotinic acetylcholine $\alpha4\beta2$ receptors: unique role of halogen bonding revealed. *J. Biol. Chem.* **287,** 4248–4259
23. Mirza, N. R., Larsen, J. S., Mathiasen, C., Jacobsen, T. A., Munro, G., Erichsen, H. K., Nielsen, A. N., Troelsen, K. B., Nielsen, E. Ø., and Ahring, P. K. (2008) NS11394 [3′-[5-(1-hydroxy-1-methyl-ethyl)-benzoimidazol-1-yl]-biphenyl-2-carbonitrile], a unique subtype-selective GABAA receptor positive allosteric modulator: *in vitro* actions, pharmacokinetic properties and *in vivo* anxiolytic efficacy. *J. Pharmacol. Exp. Ther.* **327,** 954–968
24. Celie, P. H., van Rossum-Fikkert, S. E., van Dijk, W. J., Brejc, K., Smit, A. B., and Sixma, T. K. (2004) Nicotine and carbamylcholine binding to nicotinic acetylcholine receptors as studied in AChBP crystal structures. *Neuron* **41,** 907–914
25. Winn, M. D., Ballard, C. C., Cowtan, K. D., Dodson, E. J., Emsley, P., Evans, P. R., Keegan, R. M., Krissinel, E. B., Leslie, A. G., McCoy, A., McNicholas, S. J., Murshudov, G. N., Pannu, N. S., Potterton, E. A., Powell, H. R., Read, R. J., Vagin, A., and Wilson, K. S. (2011) Overview of the CCP4 suite and current developments. *Acta Crystallogr. D Biol. Crystallogr.* **67,** 235–242
26. Zwart, P. H., Afonine, P. V., Grosse-Kunstleve, R. W., Hung, L. W., Ioerger, T. R., McCoy, A. J., McKee, E., Moriarty, N. W., Read, R. J., Sacchettini, J. C., Sauter, N. K., Storoni, L. C., Terwilliger, T. C., and Adams, P. D. (2008) Automated structure solution with the PHENIX suite. *Methods Mol. Biol.* **426,** 419–435
27. Ussing, C. A., Hansen, C. P., Petersen, J. G., Jensen, A. A., Rohde, L. A., Ahring, P. K., Nielsen, E. Ø., Kastrup, J. S., Gajhede, M., Frølund, B., and Balle, T. (2013) Synthesis, pharmacology, and biostructural characterization of novel $\alpha4\beta2$ nicotinic acetylcholine receptor agonists. *J. Med. Chem.* **56,** 940–951
28. Emsley, P., and Cowtan, K. (2004) Coot: model-building tools for molecular graphics. *Acta Crystallogr. D Biol Crystallogr.* **60,** 2126–2132
29. Sali, A., and Blundell, T. L. (1993) Comparative protein modelling by satisfaction of spatial restraints. *J. Mol. Biol.* **234,** 779–815
30. Shen, M. Y., and Sali, A. (2006) Statistical potential for assessment and prediction of protein structures. *Protein Sci.* **15,** 2507–2524
31. Jacobson, M. P., Friesner, R. A., Xiang, Z., and Honig, B. (2002) On the role of the crystal environment in determining protein side-chain conformations. *J. Mol. Biol.* **320,** 597–608
32. Brejc, K., van Dijk, W. J., Klaassen, R. V., Schuurmans, M., van Der Oost, J., Smit, A. B., and Sixma, T. K. (2001) Crystal structure of an ACh-binding protein reveals the ligand-binding domain of nicotinic receptors. *Nature* **411,** 269–276
33. Hansen, S. B., and Taylor, P. (2007) Galanthamine and noncompetitive inhibitor binding to ACh-binding protein: evidence for a binding site on non-α-subunit interfaces of heteromeric neuronal nicotinic receptors. *J. Mol. Biol.* **369,** 895–901
34. Shahsavar, A., Kastrup, J. S., Nielsen, E. Ø., Kristensen, J. L., Gajhede, M., and Balle, T. (2012) Crystal structure of Lymnaea stagnalis AChBP complexed with the potent nAChR antagonist DHβE suggests a unique mode of antagonism. *PLoS One* **7,** e40757

35. Talley, T. T., Harel, M., Hibbs, R. E., Radic, Z., Tomizawa, M., Casida, J. E., and Taylor, P. (2008) Atomic interactions of neonicotinoid agonists with AChBP: molecular recognition of the distinctive electronegative pharmacophore. *Proc. Natl. Acad. Sci. U.S.A.* **105,** 7606–7611
36. Olsen, J. A., Balle, T., Gajhede, M., Ahring, P. K., and Kastrup, J. S. (2014) Molecular recognition of the neurotransmitter acetylcholine by an acetylcholine binding protein reveals determinants of binding to nicotinic acetylcholine receptors. *PLoS One* **9,** e91232
37. Xiu, X., Puskar, N. L., Shanata, J. A., Lester, H. A., and Dougherty, D. A. (2009) Nicotine binding to brain receptors requires a strong cation-π interaction. *Nature* **458,** 534–537
38. Gallivan, J. P., and Dougherty, D. A. (1999) Can lone pairs bind to a π system? The water·hexafluorobenzene interaction. *Org. Lett.* **1,** 103–105
39. Rayes, D., De Rosa, M. J., Sine, S. M., and Bouzat, C. (2009) Number and locations of agonist binding sites required to activate homomeric Cys loop receptors. *J. Neurosci.* **29,** 6022–6032
40. Neubig, R. R., Spedding, M., Kenakin, T., and Christopoulos, A. (2003) International Union of Pharmacology Committee on Receptor Nomenclature and Drug Classification. XXXVIII. Update on terms and symbols in quantitative pharmacology. *Pharmacol. Rev.* **55,** 597–606
41. Seo, S., Henry, J. T., Lewis, A. H., Wang, N., and Levandoski, M. M. (2009) The positive allosteric modulator morantel binds at noncanonical subunit interfaces of neuronal nicotinic acetylcholine receptors. *J. Neurosci.* **29,** 8734–8742
42. Bergmann, R., Kongsbak, K., Sørensen, P. L., Sander, T., and Balle, T. (2013) A unified model of the GABA(A) receptor comprising agonist and benzodiazepine binding sites. *PLoS One* **8,** e52323